

Structure of shells in complex networks

Jia Shao¹, Sergey V. Buldyrev^{2,1}, Lidia A. Braunstein^{3,1},
Shlomo Havlin⁴, and H. Eugene Stanley¹

¹*Center for Polymer Studies and Department of Physics,
Boston University, Boston, Massachusetts 02215, USA*

²*Department of Physics, Yeshiva University,
500 West 185th Street, New York, New York 10033, USA*

³*Instituto de Investigaciones Físicas de Mar del Plata (IFIMAR)-Departamento de Física,
Facultad de Ciencias Exactas y Naturales,*

Universidad Nacional de Mar del Plata-CONICET,

Funes 3350, (7600) Mar del Plata, Argentina

⁴*Minerva Center and Department of Physics,
Bar-Ilan University, 52900 Ramat-Gan, Israel*

(Dated: Revised: October 29, 2018)

Abstract

In a network, we define shell ℓ as the set of nodes at distance ℓ with respect to a given node and define r_ℓ as the fraction of nodes outside shell ℓ . In a transport process, information or disease usually diffuses from a random node and reach nodes shell after shell. Thus, understanding the shell structure is crucial for the study of the transport property of networks. We study the statistical properties of the shells from a randomly chosen node. For a randomly connected network with given degree distribution, we derive analytically the degree distribution and average degree of the nodes residing outside shell ℓ as a function of r_ℓ . Further, we find that r_ℓ follows an iterative functional form $r_\ell = \phi(r_{\ell-1})$, where ϕ is expressed in terms of the generating function of the original degree distribution of the network. Our results can explain the power-law distribution of the number of nodes B_ℓ found in shells with ℓ larger than the network diameter d , which is the average distance between all pairs of nodes. For real world networks the theoretical prediction of r_ℓ deviates from the empirical r_ℓ . We introduce a network correlation function $c(r_\ell) \equiv r_{\ell+1}/\phi(r_\ell)$ to characterize the correlations in the network, where $r_{\ell+1}$ is the empirical value and $\phi(r_\ell)$ is the theoretical prediction. $c(r_\ell) = 1$ indicates perfect agreement between empirical results and theory. We apply $c(r_\ell)$ to several model and real world networks. We find that the networks fall into two distinct classes: (i) a class of *poorly-connected* networks with $c(r_\ell) > 1$, which have larger average distances compared with randomly connected networks with the same degree distributions; and (ii) a class of *well-connected* networks with $c(r_\ell) < 1$. Examples of poorly-connected networks include the Watts-Strogatz model and networks characterizing human collaborations, which include two citation networks and the actor collaboration network. Examples of well-connected networks include the Barabási-Albert model and the Autonomous System (AS) Internet network.

I. INTRODUCTION AND RECENT WORK

Many complex systems can be described by networks in which the nodes are the elements of the system and the links characterize the interactions between the elements. One of the most common ways to characterize a network is to determine its degree distribution. A classical example of a network is the Erdős-Rényi (ER) [1, 2] model, in which the links are randomly assigned to randomly selected pairs of nodes. The degree distribution of the ER model is characterized by a Poisson distribution

$$P(k) = \exp(-\langle k \rangle) \langle k \rangle^k / k!, \quad (1)$$

where $\langle k \rangle$ is the average degree of the network. Another simple model is a random regular (RR) graph in which each node has exactly $\langle k \rangle = \psi$ links, thus $P(k) = \delta(k - \psi)$. The Watts-Strogatz model (WS) [3] is also well-studied, where a random fraction β of links from a regular lattice with $\langle k \rangle = \psi$ are rewired and connect any pair of nodes. Changing β from 0 to 1, the WS network interpolates between a regular lattice and an ER graph. In the last decade, it has been realized that many social, computer, and biological networks can be approximated by scale-free (SF) models with a broad degree distribution characterized by a power law

$$P(k) \sim k^{-\lambda}, \quad (2)$$

with a lower and upper cutoff, k_{\min} and k_{\max} [4, 5, 6, 7, 8, 9]. A paradigmatic model that explains the abundance of SF networks in nature is the preferential attachment model of Barabási and Albert (BA)[4].

The degree distribution is not sufficient to characterize the topology of a network. Given a degree distribution, a network can have very different properties such as clustering and degree-degree correlation. For example, the network of movie actors [4] in which two actors are linked if they play in the same movie, although characterized by a power-law degree distribution, has higher clustering coefficient compared to the SF network generated by Molloy-Reed algorithm [10] with the same degree distribution.

Besides the degree distribution and clustering coefficient, a network is also characterized by the average distance between all pairs of nodes, which we refer to as the network diameter d . Random networks with a given degree distribution can be “small worlds” [2]

$$d \sim \ln N \quad (3)$$

or “ultra-small worlds” [8]

$$d \sim \ln \ln N. \quad (4)$$

The diameter d depends sensitively on the network topology.

Another important characteristic of a network is the structure of its shells, where shell ℓ is defined as the set of nodes that are at distance ℓ from a randomly chosen root node [11]. The shell structure of a network is important for understanding the transport properties of the network such as the epidemic spread [12], where the virus spread from a randomly chosen root and reach nodes shell after shell. The structure of the shells is related to both the degree distribution and the network diameter. The shell structure of SF networks has been recently studied Ref. [11], which have introduces a new term “network tomography” referring to various properties of shells such as the number of nodes and open links in shell ℓ , the degree distribution, and the average degree of the nodes in the exterior of shell ℓ .

Many real and model networks have fractal properties while others are not [13]. Recently Ref. [14] reported a power law distribution of number of nodes B_ℓ in shell $\ell > d$ from a randomly chosen root. They found that a large class of models and real networks although not fractals on all scales exhibit fractal properties in boundary shells with $\ell > d$. Here we will develop a theory to explain these findings.

II. GOALS OF THIS WORK

In this paper, we extend the study of network tomography describing the shell structure in a randomly connected network with an arbitrary degree distribution using generating functions. Following Ref. [11], we denote the fraction of nodes at distance equal to or larger than ℓ as

$$r_\ell \equiv 1 - \frac{1}{N} \sum_{m=0}^{\ell-1} B_m, \quad (5)$$

and the nodes at distances equal or larger than ℓ as the exterior E_ℓ of shell ℓ . Similarly, we define the “ r -exterior”, E_r , as the rN nodes with the largest distances from a given root node. To this end, we list all the nodes in ascending order of their distances from the root node. In this list, the nodes with the same distance are positioned at random. The last rN nodes in this list which have the largest distance to the root are called the E_r . Notice that $E_r = E_\ell$ if $r = r_\ell$. Introducing r as a continuous variable is a new step compared to

Ref.[11], which allows us to apply the apparatus of generating functions to study network tomography.

The behavior of B_ℓ for $\ell < d$ can be approximated by a branching process [15]. In shells with $\ell > d$, the network will show different topological characteristics compared to shells with $\ell < d$. This is due to the high probability to find high degree nodes (“hubs”) in shells with $\ell < d$, so there is a depletion of high degree nodes in the degree distribution in E_ℓ with $\ell > d$. Indeed, the average degree of the nodes in shells with $\ell < d$ is greater than the average degree in the shells with $\ell > d$ [11, 14].

Here, we develop a theory to explain the behavior of the degree distribution $P_r(k)$ in E_r and the behavior of the average degree $\langle k(r) \rangle$ as a function of r in a randomly connected network with a given degree distribution. Further, we derive analytically $r_{\ell+1}$ as a function of r_ℓ , $r_{\ell+1} = \phi(r_\ell)$, where ϕ can be expressed in terms of generating functions [19] of the degree distribution of the network. Using these derived analytical expressions, we explain the power law distribution $P(B_\ell) \sim B_\ell^{-2}$ for $\ell \gg d$ found in [14]. Further, based on our approach, we introduce the network correlation function $c(r_\ell) = r_{\ell+1}/\phi(r_\ell)$ to characterize the correlations in the network. We apply this measure to several model and real-world networks. We find that the networks fall into two distinct classes: a class of poorly-connected networks with $c(r_\ell) > 1$, where the virus spreads from a given root slower than in randomly connected networks with the same degree distribution; a class of well-connected networks with $c(r_\ell) < 1$, in which the virus spreads faster than in a randomly connected network.

In this paper we study RR, ER, SF, WS and BA models, as well as several real networks including the Actor collaboration network (Actor) [4], High Energy Physics citations network (HEP) [16], the Supreme Court Citation network (SCC) [17] and Autonomous System (AS) Internet network (DIMES) [18]. As we will show later, WS, Actor, HEP, and SCC belong to the class of poorly-connected networks ($c(r_\ell) > 1$), while BA model and DIMES network belong to the class of well-connected networks ($c(r_\ell) < 1$).

The paper is organized as follows. In Sec. III, we derive analytically the degree distribution and average degree of nodes in E_r and test our theory on ER and SF networks. In Sec. IV, we derive analytically a deterministic iterative functional form for r_ℓ . In Sec. V, we apply our theory to explain the distribution and average value of the number of nodes in shells. In Sec. VI, we introduce the network correlation function and apply it to different networks. Finally, we present summary in Sec. VII.

III. DEGREE DISTRIBUTION OF NODES IN r -EXTERIOR E_r

A. Generating function for $P(k)$

The generating function of a given degree distribution $P(k)$ is defined as [15, 19, 20, 21],

$$G_0(x) \equiv \sum_{k=0}^{\infty} P(k)x^k. \quad (6)$$

It follows from Eq.(6) that the average degree of the network $\langle k \rangle = G'_0(1)$. Following a randomly chosen link, the probability of reaching a node with k outgoing links (the degree of the node is $k + 1$) is

$$\tilde{P}(k) = (k + 1)P(k + 1) / \sum_{k=0}^{\infty} [(k + 1)P(k + 1)]. \quad (7)$$

Notice that

$$\sum_{k=0}^{\infty} (k + 1)x^k P(k + 1) = \sum_{k=1}^{\infty} kx^{k-1} P(k) = G'_0(x)$$

and

$$\sum_{k=0}^{\infty} (k + 1)P(k + 1) = G'_0(1) = \langle k \rangle,$$

where $\langle k \rangle$ is the average degree of the network. The generating function for the distribution of outgoing links $\tilde{P}(k)$ is

$$G_1(x) = \sum_{k=0}^{\infty} \tilde{P}(k)x^k = G'_0(x) / \langle k \rangle. \quad (8)$$

The average number of *outgoing* links, also called the branching factor of the network, is

$$\tilde{k} \equiv \sum_{k=0}^{\infty} k\tilde{P}(k) = G'_1(1) = G''_0(1) / G'_0(1) = \sum_{k=0}^{\infty} \frac{k(k + 1)P(k + 1)}{\langle k \rangle} = \frac{\langle k^2 \rangle - \langle k \rangle}{\langle k \rangle}, \quad (9)$$

For ER networks, $G_0(x)$ and $G_1(x)$ have the same simple form [15],

$$G_0(x) = G_1(x) = e^{\langle k \rangle(x-1)}, \quad (10)$$

and $\tilde{k} = \langle k \rangle$.

B. Branching process

For a randomly connected network, loops can be neglected and the construction of a network can be approximated by a branching process [15, 19, 20, 21]. In such a process,

an outgoing link, no matter at which shell ℓ from the root node it starts, has the same probability $\tilde{P}(k)$ to reach a node with k outgoing links in shell $\ell + 1$. This assumption is very good when ℓ is small and the preferential selection of the nodes with large degree (hubs) in shell ℓ does not significantly deplete the probability of finding high degree nodes in the further out shells. However, for $\ell > d$, the probability of finding hubs decreases significantly, and so does the average degree $\langle k \rangle$ [11, 14]. Another limitation of the branching process as a model of a network is that it approximates a network as a tree without loops, while in a network loops are likely to form for $\ell > d$. In order to find an approach that works well for all values of ℓ , we follow Ref. [11] and introduce a modified branching process that takes into account the depletion of large degree nodes and the formation of loops.

At the beginning of the process, we have N separate nodes, and each node has k open links, where k is a random variable with a distribution $P(k)$. We start to build the network from a randomly selected node (root). At each time step, we randomly select an open link from shell ℓ of the aggregate (root and all nodes already connected to the root) and connect this open link to another open link. There are three possible ways to select another open link (see Fig. 1), which can belong to

- (i) a free node not yet connecting to the aggregate,
- (ii) a node in shell $\ell + 1$,
- (iii) a node in shell ℓ .

When all the open links from shell ℓ are connected, we will then select an open link from shell $\ell + 1$. By doing this, the aggregate keeps growing shell after shell until all open links are connected. In cases (ii) and (iii), there are chances to create parallel links (two links connecting a pair of nodes) and circular links (one link with two ends connected to the same node). For a large network with a finite branching factor \tilde{k} , such events occur with negligible probability.

We denote by $r \equiv r(t)$ [22] the fraction of distant nodes not connected to the aggregate at step t . These nodes constitute the r -exterior E_r . At the beginning of the growth process, before we start to build the first shell, $r(0) = (N - 1)/N \approx 1$. At the end of the growth process, $r(t) = r_\infty$, where r_∞ is the fraction of nodes that are not connected to the aggregate when the building process is finished, i. e., when all open links in the aggregate are used.

The process described above simulates a randomly connected network, which is a good approximation for many model and real-world networks.

C. Degree distribution and average degree of nodes in the r-exterior E_r

Let $A_r(k)$ be the number of nodes with degree k in the r-exterior E_r at time t . The probability to have a node with degree k in E_r is given by [23]

$$P_r(k) = \frac{A_r(k)}{rN}. \quad (11)$$

When we connect an open link from the aggregate to a free node (case (i)), $A_r(k)$ changes as

$$A_{r-\frac{1}{N}}(k) = A_r(k) - \frac{P_r(k)k}{\langle k(r) \rangle}, \quad (12)$$

where $\langle k(r) \rangle = \sum P_r(k)k$ is the average degree of nodes in E_r . In the limit of $N \rightarrow \infty$, Eq.(12) can be presented as the derivative of $A_r(k)$ with respect to r

$$\frac{dA_r(k)}{dr} \approx N[A_r(k) - A_{r-\frac{1}{N}}(k)] = N \frac{P_r(k)k}{\langle k(r) \rangle}. \quad (13)$$

Differentiating Eq.(11) with respect to r , and using Eq.(13), we obtain

$$-r \frac{dP_r(k)}{dr} = P_r(k) - \frac{kP_r(k)}{\langle k(r) \rangle}, \quad (14)$$

which is rigorous for $N \rightarrow \infty$. Substituting

$$f \equiv G_0^{-1}(r) \quad (15)$$

in Eq. (14), we find by direct differentiation that

$$P_f(k) = P_1(k) \frac{f^k}{G_0(f)}, \quad (16)$$

and

$$\langle k(f) \rangle = \frac{fG_0'(f)}{G_0(f)}, \quad (17)$$

is the solution satisfying Eq. (14). Notice that $P_1(k) \equiv P(k)$.

Eq. (16) and Eq. (17) are respectively the degree distribution and the average degree in E_r , as functions of f . Once we know the explicit functional form for $G_0(x)$, we can invert $G_0(x)$ to find $f = G_0^{-1}(r)$ and find analytically both $P_r(k)$ and $\langle k(r) \rangle$:

$$P_r(k) = P(k) \frac{[G_0^{-1}(r)]^k}{r}, \quad (18)$$

$$\langle k(r) \rangle = \frac{G_0^{-1}(r)G_0'(G_0^{-1}(r))}{r}. \quad (19)$$

In a network with minimum degree $k_{\min} \geq 2$, we find by Taylor expansion that

$$\langle k(r) \rangle = k_{\min} + \frac{P(k_{\min} + 1)}{P(k_{\min})^{1+\alpha}} r^\alpha + O(r^{2\alpha}), \quad (20)$$

where $\alpha \equiv 1/k_{\min}$.

For ER networks, using Eq. (10) and Eq. (17), we find

$$\langle k(r) \rangle = \ln r + \langle k \rangle. \quad (21)$$

For $0 < r \leq 1$, Eq. (16) can be rewritten as

$$P_r(k) = P(k) \frac{(\ln r / \langle k \rangle + 1)^k}{r} = e^{-\langle k(r) \rangle} \frac{\langle k(r) \rangle^k}{k!}, \quad (22)$$

which implies that the degree distribution in the distant nodes remains a Poisson distribution but with a smaller average degree $\langle k(r) \rangle$.

Next, we test our theory numerically for ER networks with $N = 10^6$ nodes and different values of $\langle k \rangle$. To obtain $P_r(k)$, we start from a randomly chosen root node, and find the nodes in E_r and their degree distribution $P_r(k)$. This process is repeated many times for different roots and different realizations. The results are shown in Fig. 2a. The symbols are the simulation results of the degree distribution in E_r for $r = 1, 0.5$ and 0.05 . The analytical results (full lines) are computed using Eq. (22). As can be seen, the theory agrees very well with the simulation results for both $r = 0.5$ and 0.05 . We compared our theory with the simulations also for other values of r and $\langle k \rangle$ and the agreement is also excellent.

For SF networks, $G_0(x)$ and $G_1(x)$ cannot be expressed as elementary functions [15]. But for a given $P(k)$, they can be written as power series of x and one can compute the expressions in Eq.(16) and Eq.(17) numerically. In order to reduce the systematic errors caused by estimating $P(k)$, we write $G_0(x)$ and $G_1(x)$ based on the $P(k)$ obtained from the simulation results instead of using its theoretical form.

We built SF networks using the Molloy-Reed algorithm [10]. In Fig. 2b, the symbols represent the simulation results for $P_r(k)$ obtained for E_r of SF network with $\lambda = 3.5$ and $r = 1, 0.5$ and 0.1 . The lines are the numerical results calculated from Eq.(16). Good agreement between the simulation results and the theoretical predictions can be seen in Fig. 2b. Other values of r and λ have also been tested with good agreement.

In Fig. 3a, we show the average degree $\langle k(r) \rangle$ in E_r as a function of r for ER networks with different values of $\langle k \rangle$. Lines representing Eq.(21) agree very well with the numerical results (symbols) even for very small r . We note that Fig. 3a shows different value of lower limit cutoff r_∞ for r , when $\langle k(r) \rangle$ is very small. As mentioned before, r_∞ is the fraction of nodes which are not connected to the aggregate at the end of the process. In the next section, we will present an equation for r_∞ .

In Fig. 3b, we present the numerical results of Eq.(17) for SF networks with different values of λ . For a given E_r , $\langle k(r) \rangle$ is computed from the simulated network and the results are averaged over many realizations. Good agreement between the theory (lines) and the simulation results (symbols) can be seen.

IV. ITERATIVE FUNCTIONAL FORM OF r_ℓ , THE FRACTION OF NODES OUTSIDE SHELL ℓ

In this section, we study the growth of the aggregate itself. Let $L(t)$ be the number of open links belonging to the full aggregate at step t , and $\Lambda(t) \equiv L(t)/N$. The number of open links belonging to shell ℓ of the aggregate is defined as $L_\ell(t)$ and $\Lambda_\ell(t) \equiv L_\ell(t)/N$. After we finish building shell ℓ and just before we start to build shell $\ell + 1$, all the open links in the aggregate belong to nodes in shell ℓ , so $t = t_\ell$, we have $\Lambda_\ell(t) = \Lambda(t)$ [24]. In the process of building shell $\ell + 1$, $\Lambda_\ell(t)$ decreases to 0.

Next we show that both $\Lambda(t)$ and $\Lambda_\ell(t)$ can be expressed as functions of r . In analogy with Eq.(9), we define the branching factor of nodes in the r -exterior E_r as

$$\tilde{k}(r) = \frac{\langle k^2(r) \rangle - \langle k(r) \rangle}{\langle k(r) \rangle} = \frac{\sum_{k=0}^{\infty} k^2 P_r(k)}{\langle k(r) \rangle} - 1. \quad (23)$$

Using Eq.(23) and Eq.(17), $\tilde{k}(r)$ can be rewritten as a function of f as

$$\tilde{k}(f) = \frac{f G_0''(f)}{G_0'(f)}. \quad (24)$$

Appendix A shows that $\Lambda(r)$ and $\Lambda_\ell(r)$ obey differential equations

$$\frac{d\Lambda(r)}{dr} = -\tilde{k}(r) + 1 + \frac{2\Lambda(r)}{r\langle k(r) \rangle} \quad (25)$$

$$\frac{d\Lambda_\ell(r)}{dr} = 1 + \frac{\Lambda(r)}{r\langle k(r) \rangle} + \frac{\Lambda_\ell(r)}{r\langle k(r) \rangle} \quad (26)$$

Eq.(25) and Eq.(26) govern the growth of the aggregate. To solve them, we make the same substitution $f = G_0^{-1}(r)$ (Eq.[15]) as before. The general form of the solution for Eq.(25) is

$$\Lambda(f) = -G'_0(f)f + C_1f^2, \quad (27)$$

where C_1 is a constant. At time $t=0$, $r = f = 1$, and $\Lambda(1) = 0$. With this initial condition, we obtain $C_1 = G'_0(1) = \langle k \rangle$. Using Eq.(27), the general solution of Eq.(26) is

$$\Lambda_\ell(f) = G'_0(1)f^2 + C_2f, \quad (28)$$

where C_2 is a constant. When $r = r_\ell$, the building of shell ℓ is finished. At that time, all the open links of the aggregate belong to shell ℓ , $\Lambda(r) |_{r=r_\ell} = \Lambda_\ell(r) |_{r=r_\ell}$. If we denote $f_\ell \equiv G_0^{-1}(r_\ell)$, $C_2 = -G'_0(f_\ell)$. Thus, the solutions of the differential equations Eqs.(25) and (26) are

$$\Lambda(f) = G'_0(1)f^2 - G'_0(f)f \quad (29)$$

$$\Lambda_\ell(f) = G'_0(1)f^2 - G'_0(f_\ell)f \quad (30)$$

When all open links in the aggregate are used, $\Lambda = 0$, the corresponding $f = f_\infty$ gives the fraction of nodes $r_\infty = G_0(f_\infty)$ which do not belong to the aggregate when the building process is finished. The value of f_∞ must satisfy Eq.(29) with $\Lambda(f_\infty) = 0$

$$f_\infty = G'_0(f_\infty)/G'_0(1) \equiv G_1(f_\infty), \quad (31)$$

and from Eq.(15)

$$r_\infty = G_0(f_\infty). \quad (32)$$

Eqs. (31) and (32) imply that there exist a certain fraction of distant links and nodes not connected to the aggregate when the building process is finished. These results are consistent with previous work [21]. The numerical solution for Eq.(31) is discussed in Sec. IV (A) and Appendix B.

When $\Lambda_\ell(f) = 0$, the construction of shell $\ell + 1$ is completed, $r = r_{\ell+1}$ and $f = f_{\ell+1}$. Then from Eq.(30), we obtain

$$f_{\ell+1} = G'_0(f_\ell)/G'_0(1) = G_1(f_\ell), \quad (33)$$

which leads to a deterministic iterative functional form for r_ℓ

$$r_{\ell+1} = G_0(f_{\ell+1}) = G_0(G_1(G_0^{-1}(r_\ell))) \equiv \phi(r_\ell). \quad (34)$$

Eq. (34) allows us to make a deterministic prediction of $r_{\ell+1}$ once we know $r_{\ell-1}$.

This result is different from a similar well-known result [19] based on the physical meaning of the generating function $G_0(r)$, which gives a fraction of nodes in the set B not directly connected to a randomly selected fraction $1 - r$ of set A. The difference with Eq.(34) is that set A is selected not by constructing shells around a root but randomly. Moreover, set B may even overlap with set A.

To test our theory, we use RR networks, where $P(k) = \delta(k - \psi)$, $G_0(x) = x^\psi$ and $G_1(x) = x^{\psi-1}$, then Eq.(34) reduces to

$$r_{\ell+1} = r_\ell^{\psi-1}, \quad (35)$$

which is shown as lines in Fig. 4a. The symbols in Fig. 4a are the simulation results for RR networks with different values of ψ . To obtain the simulation results, at each realization a random root is chosen and a full set of r_ℓ is computed. The results obtained for many realizations are plotted as a scatter plot. Due to the homogeneity of RR network, r_ℓ can only take on discrete values. The agreement between the simulation results and Eq.(35) is excellent, and the scattering almost cannot be observed [25].

For ER networks, Eq.(34) yields

$$r_{\ell+1} = e^{\langle k \rangle (r_\ell - 1)}, \quad (36)$$

which is valid for all $\ell > 1$. We test Eq.(36) for ER network with different values of $\langle k \rangle$ and the results are shown in Fig. 4b. The agreement between the theoretical predictions (lines) and the the simulation results is excellent.

For SF networks, Eq.(34) can be solved numerically using the values of $P(k)$ from the generated SF network. The lines shown in Fig. 4c represent the numerical solutions of the theory [Eq.(34)]. The symbols are the simulation results for the generated SF networks. For $\lambda \geq 2.5$, a good agreement between theory and simulation results can be seen. Note that for the very small value of $\lambda = 2.2$, the simulation results deviate slightly from the theory due to high probability of creating *parallel and circular links* (PCL) in the hubs of the randomly connected network [26] (created by case (ii) and (iii) in Fig. 1). We test Eq.(34) for a SF network of $\lambda = 2.2$ allowing PCL during its construction. The results are shown in Fig. 4d as a log-linear plot. The agreement between the theory and the simulation results for a SF network with $\lambda = 2.2$ in presence of PCL is very good. This shows that SF networks built

by the Molloy-Reed algorithm without PCL deviate from randomly connected networks for very small values of λ . We will further discuss this deviation in Sec. V B.

V. APPLICATIONS

A. Derivation of the power-law distribution of B_ℓ for $\ell \gg d$

Recently, a broad power-law distribution of the number of nodes at shell ℓ ($\ell \gg d$), B_ℓ , has been reported [14]. This power-law distribution exists in many model and real networks and is characterized by a universal form $P(B_\ell) \sim B_\ell^{-2}$ (see Fig. 5). Using Eq.(34), we will prove this relation and explain the origin of this universal power-law distribution.

For the purpose of clarity, we use m instead of ℓ for shells with $\ell < d$, and n instead of ℓ for $\ell > d$. For the entire range of shell indices, ℓ will be used.

For infinitely large networks, we can neglect loops for $\ell < d$ and approximate the forming of a network as a branching process [15, 19, 20, 21]. It has been reported [15, 20] that for shell m (with $m \ll d$), the generating function for the number of nodes, B_m , in the shell m is

$$\tilde{G}_m(x) = G_0(G_1(\dots(G_1(x)))) = G_0(G_1^{m-1}(x)), \quad (37)$$

where $G_1(G_1(\dots)) \equiv G_1^{m-1}(x)$ is the result of applying $G_1(x)$, $m - 1$ times and $P(B_m)$ is the coefficient of x^{B_m} in the Taylor expansion of $\tilde{G}_m(x)$ around $x = 0$. The average number of nodes in shell m is \tilde{k}^m [15]. It is possible to show that $G_1^m(x)$ converges to a function of the form $\Phi((1-x)\tilde{k}^m)$ for large m [20], where $\Phi(x)$ satisfies the Poincaré functional relation

$$G_1(\Phi(y)) = \Phi(y\tilde{k}), \quad (38)$$

where $y \equiv 1 - x$. The functional form of $\Phi(y)$ can be uniquely determined from Eq.(38).

It is known that $\Phi(y)$ has an asymptotic functional form, $\Phi(y) = f_\infty + ay^{-\delta} + o(y^{-\delta})$, where a is a constant [20]. Expanding both sides of Eq.(38), we obtain

$$G_1(f_\infty) + G_1'(f_\infty)ay^{-\delta} = f_\infty + a\tilde{k}^{-\delta}y^{-\delta} + o(y^{-\delta}). \quad (39)$$

Since $G_1(f_\infty) = f_\infty$, we find

$$\delta = -\ln G_1'(f_\infty) / \ln \tilde{k}. \quad (40)$$

The numerical solution of $G_1(f_\infty) = f_\infty$ depends on different scenarios (see Appendix B) as

$$f_\infty \begin{cases} > 0, & \text{for } P(k=1) \neq 0; \\ = 0, & \text{for } P(k=1) = 0. \end{cases} \quad (41)$$

The solution for δ is (see Appendix B)

$$\delta \begin{cases} > 0, & \text{for } P(k=1) \neq 0 \text{ and } P(k=2) \neq 0; \\ = \infty, & \text{for } P(k=1) = 0 \text{ and } P(k=2) = 0. \end{cases}$$

Applying Tauberian-like theorems [20, 27] to $\Phi(y)$, which has a power-law behavior for $y \rightarrow \infty$, the Taylor expansion coefficient of $\tilde{G}_m(x)$, it has been found [27] that $P(B_m)$ behaves as B_m^μ with an exponential cutoff at $B_m^* \sim \tilde{k}^m$ and some quasi-periodic modulations with period 1 as a function of $\log_{\tilde{k}} B_m$ [20, 27], where

$$\mu = \begin{cases} \delta - 1, & \text{for } P(k=1) \neq 0; \\ 2\delta - 1, & \text{for } P(k=1) = 0 \text{ and } P(k=2) \neq 0; \\ \infty, & \text{for } P(k=1) = 0 \text{ and } P(k=2) = 0. \end{cases}$$

Thus, the probability distribution of the number of nodes in the shell m has a power law tail for small values of B_m [14],

$$P(B_m) \sim B_m^\mu, \quad (42)$$

if $P(k=1) + P(k=2) > 0$.

The above considerations are correct only for $m \ll d$, where the depletion of nodes with large degree is insignificant. For $\ell > d$, we must consider the changing of $P_r(k)$.

Using Eq.(34) for the whole range of ℓ , we can write the relation between r_n for $n > d$ and r_m for $m \ll d$ as

$$r_n = G_0(G_1(G_0^{-1}(G_0(G_1(G_0^{-1} \dots (r_m) \dots))) = G_0(G_1^{n-m}(G_0^{-1}(r_m))) = G_0(G_1^{n-m}(f_m)). \quad (43)$$

Applying the same considerations as for B_m , we obtain,

$$G_1^{n-m}(f_m) = f_\infty + a\tilde{k}^{-\delta(n-m)}(1 - f_m)^{-\delta}. \quad (44)$$

Using

$$1 - f_m = 1 - G_0^{-1}(r_m) = 1 - G_0^{-1}(1 - (1 - r_m)), \quad (45)$$

we can write a Taylor expansion for $z \equiv 1 - r_m$ as

$$1 - f_m = 1 - G_0^{-1}(1 + z) \approx 1 - [1 - z(G_0^{-1})'(1)] = z/\langle k \rangle. \quad (46)$$

Thus, we obtain

$$G_1^{n-m}(f_m) \approx f_\infty + a \left[\frac{\tilde{k}^{n-m}}{\langle k \rangle} (1 - r_m) \right]^{-\delta}. \quad (47)$$

Applying G_0 on both sides of Eq.(47) and using Taylor expansion, we obtain

$$r_n = G_0(f_\infty) + G_0'(f_\infty)\zeta + \frac{G_0''(f_\infty)}{2}\zeta^2 \dots, \quad (48)$$

where $\zeta \equiv a(\tilde{k}^{n-m}/\langle k \rangle)^{-\delta}(1 - r_m)^{-\delta}$. If $P(k=1) \neq 0$, as discussed in Eq.(41) and Appendix B, f_∞ is non-zero, $G_0'(f_\infty) = \langle k \rangle G_1(f_\infty) = \langle k \rangle f_\infty$ is also non-zero, thus we can ignore the ζ^2 term and keep the leading non-zero term ζ . If $P(k=1) = 0$ and $P(k=2) \neq 0$, both $G_1(f_\infty)$ and f_∞ are zero, $G_0''(f_\infty) = \langle k \rangle G_1'(0) = 2P(k=2) \neq 0$ and then $\frac{G_0''(f_\infty)}{2}\zeta^2$ is the leading non-zero term. Thus,

$$r_n - r_\infty \approx a f_\infty \frac{\tilde{k}^{\delta(n-m)}}{\langle k \rangle^{-\delta-1}} (1 - r_m)^{-\delta} \approx (1 - r_m)^{-\mu-1}, \quad P(k=1) \neq 0 \quad (49)$$

$$r_n - r_\infty \approx P(2)a^2 \left[\frac{\tilde{k}^{n-m}(1 - r_m)}{\langle k \rangle} \right]^{-2\delta} \approx (1 - r_m)^{-\mu-1}, \quad P(k=1) = 0, P(k=2) \neq 0 \quad (50)$$

Since B_ℓ increases exponentially with ℓ for $\ell < d$ and decreases even faster than exponentially for $\ell > d$ [15], we can make approximations $r_n \sim B_n/N$ and $1 - r_m \sim B_m/N$ for $n \gg d$ and $m \ll d$ respectively. Using $P(B_n)dB_n = P(B_m)dB_m$ and Eqs.(42), (49) and (50), we obtain

$$P(B_n) \sim B_n^{-1-\mu/(\mu+1)-1/(\mu+1)} = B_n^{-2}, \quad (51)$$

which is valid for $n \gg d$.

The power-law distribution shown by Eq.(51) indicates that fractal features exist at the boundaries of almost all networks. Further studies of these fractal features are represented in Ref. [14].

B. Average number of nodes in shell ℓ , $\langle B_\ell \rangle$

The number of nodes in shell ℓ can be expressed as a function of r_ℓ as

$$B_\ell = N(r_\ell - r_{\ell+1}). \quad (52)$$

From Eq.(34) and Eq.(52), with initial condition $r = r_m$, one can calculate B_ℓ for all $\ell \geq m$ and find $\langle B_\ell \rangle$ for $\ell \geq m$ using $P(B_\ell)$.

However, when we study a finite network, the effect of the first few shells needs to be considered. Take a RR network as an example. From simulation data it is clear that $B_0 = 1$, $B_1 = \psi$ and $B_2 = \psi(\psi - 1)$, and correspondingly $r_1 = 1 - 1/N$, $r_2 = 1 - (\psi + 1)/N$ and $r_3 = 1 - (1 + \psi + \psi(\psi - 1))/N = 1 - (\psi^2 + 1)/N$. If we apply Eq.(35) on r_1 and r_2 , the calculated $r_2 = 1 - (\psi - 1)/N$ and $r_3 = 1 - (\psi^2 - 1)/N$ deviate from the simulated results of r_2 and r_3 by a constant value of $2/N$. For $N \rightarrow \infty$ and large ℓ , this deviation is negligible. However for a finite system and small ℓ , we have to consider this term. To cancel this constant deviation, we modify Eq.(35) as

$$r_{\ell+1} = r_{\ell}^{\psi-1} - 2/N. \quad (53)$$

Using Eq. (53), starting from r_1 , we can calculate r_{ℓ} and B_{ℓ} for any $\ell > 1$. For RR network, due to the homogeneity of the degree, the distribution of B_{ℓ} is a delta function, thus $\langle B_{\ell} \rangle = B_{\ell}$. In Fig. 6, we show the theoretical predictions of $\langle B_{\ell} \rangle$ (full lines) together with the simulation results (symbols) for different values of ψ . The simulation results are the average over different realizations. The agreement between the theory and the simulation results is excellent.

For networks with varying degree (like ER and SF), $\langle B_{\ell} \rangle$ cannot be directly calculated from our theory. The reason is that for these networks, the modification needed on Eq.(34) is not a constant but fluctuates with a magnitude of the order of $1/N$. Further, because $\langle \phi(r_{\ell}) \rangle \neq \phi(\langle r_{\ell} \rangle)$, we cannot replace B_{ℓ} with $\langle B_{\ell} \rangle$ as we did for RR. As we see in Fig. 4, Eq.(34) works well also for varying degree networks in predicting $r_{\ell+1}$ once r_{ℓ} is known. It also works well in predicting $B_{\ell+\Delta}$ ($\Delta = 1, 2, 3, \dots$) given a shell with big enough B_{ℓ} ($\approx 10^4$). It can reproduce the behavior of successive shells with 99% accuracy. However, when $B_{\ell+\Delta}$ become small ($< 10^4$), the error is relatively large.

VI. THE NETWORK CORRELATION FUNCTION $c(r)$

In this section we will compare various models and real-world networks with the randomly connected networks with same degree distributions and introduce a new network characteristic, the network correlation function $c(r)$ analogous to the density correlation function in statistical mechanics [29]. For a randomly connected network, $c(r) = 1$, as for the density correlation function in the ideal gas, while for the non-random networks the deviation of

$c(r)$ from unity characterizes their correlations on different distances from the root.

A. SF networks with $\lambda \leq 3$

Our theory crucially depends on the existence of the branching factor \tilde{k} . So we can expect significant deviations from our theory in the behavior of the SF networks with $\lambda \leq 3$, for which \tilde{k} diverges for $N \rightarrow \infty$. However, for a fixed N , the degree distribution is truncated by the natural cutoff $k_{\max} \sim N^{1/(\lambda-1)}$, so that \tilde{k} still exists. Hence, we hypothesize that our theory remains valid even for $\lambda < 3$ for randomly connected networks (with PCL) (see Fig. 7). Another problem is that our algorithm of constructing randomly connected networks leads to formation of PCL. The PCL is typically forbidden in the construction algorithms of the network characterizing complex systems. In order to construct a network without PCL, one imposes significant correlations in network structure of a dissortative nature with greater probability of hubs to be connected to small degree nodes than in a randomly connected network [26]. Thus, we can predict that SF networks with $\lambda \leq 3$ which do not include PCL must significantly deviate from the prediction of our theory.

In order to characterize this deviation we define a correlation function

$$c(r_\ell) \equiv r_{\ell+1}/\phi(r_\ell), \quad (54)$$

where $r_{\ell+1}$ and r_ℓ characterize two successive shells of a network under investigation while $\phi(r_\ell)$ is the prediction (Eq.(34)) of $r_{\ell+1}$ based on our theory for a randomly connected network. Accordingly, we compute $c(r_\ell)$ for several networks with $N = 10^6$ nodes with $\lambda = 2.5$ and $\lambda = 2.2$, for the randomly connected case and for the case in which PCL are not allowed. We find in Fig. 7 that for randomly connected networks $c(r_\ell)$ is always close to 1 with the expected random deviations for $r_\ell \rightarrow 0$ and $r_\ell \rightarrow 1$ caused by random fluctuations in the small first ($r_\ell \rightarrow 1$) and last ($r_\ell \rightarrow 0$) shells. In contrast, $c(r_\ell)$ is uniformly smaller than 1 for the networks without PCL. For $\lambda = 2.5$ the deviations are small because the typical number of PCL that would randomly form still constitute a negligible fraction of links. For $\lambda = 2.2$ the deviations are significant because in this case the chance of formation of PCL is much higher. In both cases, the deviation are increasing with the maximal degree of the network, which can randomly fluctuate around its average value $k_{\min} N^{1/(\lambda-1)} \Gamma[(\lambda-2)/(\lambda-1)]$ [28]. The value of $c < 1$ for these networks indicates the fact that due to the absence of

PCL more nodes are attached to the next shells compared to randomly connected networks. Accordingly, for such networks, the fraction of nodes not included into shell $\ell + 1$ is smaller than that in randomly connected networks. Thus, SF networks for $\lambda < 3$ are dissortative, which means that the degree of a node is anti-correlated with the average degree of its neighbors. Moreover, these anti-correlations are barely visible for $\lambda > 2.5$ and increase with the decrease of λ . Therefore $c(r_\ell) < 1$ can be associated with the network dissortativeness.

B. Global measurement of correlations

The network building process described in Sec. II corresponds to a randomly connected network for a given $P(k)$. However, real-world and model networks do not always follow the behavior described by our theory. The correlation function $c(x)$ constructed in the previous section [Eq. (34)] can be used to detect non-randomness in the network connections.

For a given degree distribution, we define poorly-connected networks as those in which $c(r_\ell) > 1$. Conversely, we define well-connected networks as those in which $c(r_\ell) < 1$. The motivation for this definition is that if $c(r_\ell) > 1$, it means that the number of nodes in shell ℓ , $B_\ell = N(r_\ell - r_{\ell+1}) = N[r_\ell - c(r_\ell)\phi(r_\ell)]$, is smaller than $N[r_\ell - \phi(r_\ell)]$, the value expected for a randomly connected network with the same degree distribution. Therefore in a poorly-connected network information or virus spreads slower than in a randomly connected network in accordance with the meaning of the term poorly-connected. Conversely, in well-connected networks information spreads faster than in randomly connected network with the same degree distribution. Poorly-connected networks usually contain cliques of fully connected nodes. In a clique, the majority of links connect back to the already connected nodes in shell ℓ . So the new shell $\ell + 1$ grows slower than for a randomly connected network with the same degree distribution.

As an example, we analyze the WS model characterized by high clustering. In this case the number of links which can be used to build the next shell of neighbors is much smaller than in a randomly connected network with the same degree distribution. Thus we can expect $c > 1$ in particular for a small fraction β of rewired links (see Fig. 8a). Further, we find that the networks characterizing human collaborations are usually poorly connected (see Fig. 8b). A typical example of such a network is the actor network, where a link between two actors indicates that they play in the same movie at least once. So all the

actors played in the same movie form a fully connected subset of the network (“clique”). As a result, the majority of their links are not used to attract new actors but circle back to the previously acquainted actors. The same is correct for the Supreme Court Citation network (SCC) and High Energy Physics citations (HEP) networks in Fig. 8b. Actor, HEP, and SCC networks all contain a large amount of highly inter-connected cliques. As we see these cliques manifests themselves in $c > 1$. In contrast the DIMES network [18], is designed to be well-connected and as a result it has $c < 1$.

Another example of a well-connected network is the BA model, in which $c(r_\ell)$ linearly goes to zero for $r_\ell \rightarrow 0$ [Fig. 8(c)]. In the BA model a new node, which has exactly k_{\min} open links, randomly attaches its links to the previously existing nodes with probabilities proportional to their current degrees. (PCL are forbidden.) One can see that for $k_{\min} \geq 2$, $c(r_\ell) < 1$ for all r_ℓ except in a small vicinity of $r_\ell = 1$. This fact is associated with the dissortative nature of the BA model, in which small degree nodes that are created at the late stages of the network construction are connected with very high probability to the hubs that are created at the early stages. Thus as soon as the hubs are reached during shell construction, the rest of the nodes can be reached much faster than in a randomly connected network.

The small region of $c(r_\ell) > 1$ for $r_\ell \rightarrow 1$ can be associated with the fact that the hubs which are created at the early stages of the BA network construction, are not necessarily directly connected to each other as it would be in randomly connected networks. Thus initial shells of the BA model corresponding to large r_ℓ grow slower than they would grow in the randomly connected network. The effect is especially strong for $k_{\min} = 1$ in which the BA network is a tree, and the distance between certain hubs can be quite large. Thus BA with $k_{\min} = 1$ gives an example of a network with poor connectivity between the hubs (large $r_\ell \rightarrow 1$) and good connectivity among the low degree nodes ($r_\ell \rightarrow 0$) which are directly connected to the hubs. In a network in which long connected chains of low degree nodes are abundant, we will have poor connectivity ($c(r_\ell) > 1$) for $r_\ell \rightarrow 0$. In general, the behavior of $c(r_\ell)$ for $r_\ell \rightarrow 1$ characterizes the connectivity among the hubs, while the behavior of $c(r_\ell)$ for $r_\ell \rightarrow 0$ characterizes the connectivity among the low-degree nodes.

VII. SUMMARY

In this paper, we derive new analytical relations describing shell properties of a randomly connected network. In particular, we expand the results of Ref. [11] on the network tomography using the apparatus of the generating functions. We find how the degree distribution is depleted as we approach the boundaries of the network which consist of the r -fraction of nodes which are most distant from a root node. We find an explicit analytical expression for the degree distribution as a function of r [Eqs. (16) and (17)]. We also derive an explicit analytical relation between the values of r for two successive shells ℓ and $\ell + 1$ [Eq.(34)]. Using this equation we construct a correlation function $c(r)$ [Eq.(54)] of the network which characterizes the quality of the network connectedness. We apply this measure for several model and real networks. We find that human collaboration networks are usually poorly-connected compared to the random networks with the same degree distribution. The same is true for the WS small-world model. In contrast, we find that the Internet is a well-connected network. The same is true for the BA model. Thus our results indicate that the WS model and the BA model correctly reproduce an essential feature of the real-world models they were designed to mimic, namely, social networks and the Internet, respectively. Finally we apply Eq. (34) to derive the power law distribution of the number of nodes in the shells with $\ell \gg d$ [14].

VIII. ACKNOWLEDGMENTS

We wish to thank the ONR, EU project Epiwork, the Israel Science Foundation for financial support. S.V.B. thanks the Office of the Academic Affairs of Yeshiva University for funding the Yeshiva University high performance computer cluster and acknowledges the partial support of this research through the Dr. Bernard W. Gamson Computational Science Center at Yeshiva College.

APPENDIX A: DIFFERENTIAL EQUATIONS FOR $\Lambda(r)$ AND $\Lambda_\ell(r)$

In this appendix, we derive the differential equations (Eq. (25)) for $\Lambda(t)$ and $\Lambda_\ell(t)$. At time t , the total number of open links in the r -exterior E_r of the unconnected nodes is $rN\langle k(r) \rangle$. At step t , we connect one open link from the aggregate to another open link.

There is a probability

$$\frac{r(t)\langle k(r(t))\rangle}{r(t)\langle k(r(t))\rangle + \Lambda(t)}$$

that will be connected to a free node. Thus,

$$Nr(t+1) = Nr(t) - \frac{r(t)\langle k(r(t))\rangle}{r(t)\langle k(r(t))\rangle + \Lambda(t)}. \quad (\text{A1})$$

To derive the differential equations for $\Lambda(t)$, we need to consider all three different scenarios which we illustrated in Fig. 1. If we connect an open link from the aggregate to a node which is not yet connected to the aggregate (scenario (i) in Fig. 1), on average $\Lambda(t)$ will increase by $\tilde{k}(r(t))/N$. If we connect the open link from the aggregate to another open link either from shell ℓ or shell $\ell+1$ (scenarios (iii) and (ii) in Fig. 1), $\Lambda(t)$ will decrease by $1/N$. Because we connect links at random, the probability of scenario (i) is

$$\frac{r(t)\langle k(r(t))\rangle}{r(t)\langle k(r(t))\rangle + \Lambda(t)}$$

and the probability of scenarios (ii) or (iii) is

$$\frac{\Lambda(t)}{r(t)\langle k(r(t))\rangle + \Lambda(t)}.$$

Thus, we can write down the evolution of $\Lambda(t)$ as

$$\Lambda(t+1) = \Lambda(t) - \frac{1}{N} + \frac{\tilde{k}(r(t))}{N} \frac{r(t)\langle k(r(t))\rangle}{r(t)\langle k(r(t))\rangle + \Lambda(t)} - \frac{1}{N} \frac{\Lambda(t)}{r(t)\langle k(r(t))\rangle + \Lambda(t)}. \quad (\text{A2})$$

For $N \rightarrow \infty$, Eqs. (A1) and (A2) lead respectively to

$$\frac{dr(t)}{dt} = -\frac{1}{N} \frac{r(t)\langle k(r(t))\rangle}{r(t)\langle k(r(t))\rangle + \Lambda(t)}, \quad (\text{A3})$$

and

$$\frac{d\Lambda(t)}{dt} = -\frac{1}{N} + \frac{\tilde{k}(r(t))}{N} \frac{r(t)\langle k(r(t))\rangle}{r(t)\langle k(r(t))\rangle + \Lambda(t)} - \frac{1}{N} \frac{\Lambda(t)}{r(t)\langle k(r(t))\rangle + \Lambda(t)}. \quad (\text{A4})$$

Dividing Eq.(A4) by Eq.(A3) we obtain the differential equation for Λ as a function of r

$$\frac{d\Lambda(r)}{dr} = -\tilde{k}(r) + 1 + \frac{2\Lambda(r)}{r\langle k(r)\rangle}. \quad (\text{A5})$$

$\Lambda_\ell(t)$ behaves similarly to $\Lambda(t)$ except that we only need to consider the effect of scenario (iii) of Fig. 1. Accordingly, the evolution of Λ_ℓ can be written as

$$\Lambda_\ell(t+1) = \Lambda_\ell(t) - \frac{1}{N} - \frac{1}{N} \frac{\Lambda_\ell(t)}{r(t)\langle k(r(t))\rangle + \Lambda(t)}, \quad (\text{A6})$$

which for $N \rightarrow \infty$ is

$$\frac{d\Lambda_\ell(t)}{dt} = -\frac{1}{N} - \frac{1}{N} \frac{\Lambda_\ell(t)}{r(t)\langle k(r(t)) \rangle + \Lambda(t)}. \quad (\text{A7})$$

Dividing Eq.(A7) by Eq.(A3), we get

$$\frac{d\Lambda_\ell(r)}{dr} = 1 + \frac{\Lambda(r)}{r\langle k(r) \rangle} + \frac{\Lambda_\ell(r)}{r\langle k(r) \rangle}. \quad (\text{A8})$$

APPENDIX B: SOLUTION OF $G_1(f_\infty) = f_\infty$ AND $\delta = -\ln G'_1(f_\infty)/\ln \tilde{k}$

The numerical solutions of $G_1(f_\infty) = f_\infty$ can be shown by a simple example. Suppose we have three simple networks A, B and C. In network A, all the nodes can only have degree 1, 2 and 3. In network B, the degree can be 2, 3 and 4. In network C, the degree can be 3, 4 and 5. For all three examples, the probability of each degree is $1/3$. We can write G_0 and G_1 for three network as

$$G_{0,A}(x) = \frac{1}{3}x + \frac{1}{3}x^2 + \frac{1}{3}x^3 \quad (\text{B1})$$

$$G_{0,B}(x) = \frac{1}{3}x^2 + \frac{1}{3}x^3 + \frac{1}{3}x^4 \quad (\text{B2})$$

$$G_{0,C}(x) = \frac{1}{3}x^3 + \frac{1}{3}x^4 + \frac{1}{3}x^5 \quad (\text{B3})$$

The average degrees $\langle k \rangle = G'_0$ of A, B and C are 2, 3 and 4 respectively. Using the above expressions for G_0 we can construct the expressions for $G_1(x)$:

$$G_{1,A}(x) = \frac{1}{6} + \frac{1}{3}x + \frac{1}{2}x^2 \quad (\text{B4})$$

$$G_{1,B}(x) = \frac{2}{9}x + \frac{1}{3}x^2 + \frac{4}{9}x^3 \quad (\text{B5})$$

$$G_{1,C}(x) = \frac{1}{4}x^2 + \frac{1}{3}x^3 + \frac{5}{12}x^4 \quad (\text{B6})$$

The branching factors $\tilde{k} = G'_1(1)$ of A, B and C are $2/3$, $20/9$ and $19/6$ respectively. The numerical solutions of $G_1(f_\infty) = f_\infty$ for network A and B is shown in Figs. 9a and 9b, where we plot the functions $y = f$ and $y = G_1(f)$ on the same plot. From Fig. 9, we can see that there is a non-zero $f_\infty = 1/3$ for network A and $f_\infty = 0$ for network B. For network C, we also have $f_\infty = 0$. Whether we can have a non-zero f_∞ depends on the first term of $G_1(x)$, which depends on $P(k=1)$, the probability of having nodes with degree 1. If $P(k=1) \neq 0$, we can have $f_\infty \neq 0$, if $P(k=1) = 0$, $f_\infty = 0$. Using Eq.(40), we can calculate $\delta_A = \ln(3/2)/\ln(4/3) \approx 1.41$, $\delta_B = \ln(9/2)/\ln(20/9) \approx 1.88$ and $\delta_C = \infty$. It is clear that network A and B have finite δ , while for network C, $G'_1(0) = 0$ thus $\delta_c = \infty$. In order to

have finite δ , $P(k = 2) + P(k = 1)$ must be greater than 0. If $P(k = 2) = P(k = 1) = 0$ (called the Böttcher case [20]), then $\delta = \infty$, which indicates that $\Phi(y)$ has an exponential singularity. For the Böttcher case, the distribution of B_ℓ is not described by a power law, i.e. there are no fractal boundaries.

-
- [1] P. Erdős and A. Rényi, *Publ. Math.* **6**, 290 (1959); *Publ. Math. Inst. Hung. Acad. Sci.* **5**, 17 (1960).
- [2] B. Bollobás, *Random Graphs* (Academic, London, 1985).
- [3] D. J. Watts and S. H. Strogatz, *Nature (London)* **393**, 440 (1998).
- [4] A.-L. Barabási and R. Albert, *Science* **286**, 509 (1999).
- [5] R. Albert and A.-L. Barabási, *Rev. Mod. Phys.* **74**, 47(2002).
- [6] R. Pastor-Satorras and A. Vespignani, *Evolution and Structure of the Internet: A Statistical Physics Approach* (Cambridge University Press, 2006).
- [7] S. N. Dorogovtsev and J. F. F. Mendes, *Evolution of Networks: from Biological nets to the Internet and WWW* (Oxford University Press, New York, 2003).
- [8] R. Cohen and S. Havlin, *Phys. Rev. Lett.* **90**, 058701 (2003).
- [9] R. Pastor-Satorras and A. Vespignani, *Evolution and Structure of the Internet: a statistical physics approach* (Cambridge University Press, 2006).
- [10] M. Molloy and B. Reed, *Comb. Probab. Comput.* **7**, 295 (1998).
- [11] T. Kalisky, R. Cohen, O. Mokryn, D. Dolev, Y. Shavitt, S. Havlin 537. *Phys. Rev. E* **74**, 066108 (2006).
- [12] M. E. J. Newman, *Phys. Rev E* **66**, 016128 (2002).
- [13] C. Song *et al.*, *Nature (London)* **433**, 392 (2005); *Nature Physics* **2**, 275 (2006).
- [14] J. Shao, S. V. Buldyrev, R. Cohen, M. Kitsak, S. Havlin and H. E. Stanley, *Europhys. Lett.* **84**, 48004 (2008).
- [15] M. E. J. Newman, S. H. Strogatz, and D. J. Watts, *Phys. Rev. E* **64**, 026118 (2001).
- [16] Derived from the HEP section of arxiv.org; <http://vlado.fmf.uni-lj.si/pub/networks/data/hep-th/hep-th.htm> (website of Pajek).
- [17] J. H. Fowler, S. Jeon, *Social Networks* **30**, 16 (2008).
- [18] Y. Shavitt and E. Shir, DIMES - Letting the Internet Measure Itself, <http://www.arxiv.org/abs/cs.NI/0506099>
- [19] T. E. Harris, *Ann. Math. Statist.* **41**, 474 (1948); *The Theory of Branching Processes* (Springer-Verlag, Berlin, 1963).

- [20] N. H. Bingham, *J. Appl. Probab.* **25A**, 215 (1988).
- [21] L. A. Braunstein, Z. Wu, Y. Chen, S. V. Buldyrev, T. Kalisky, S. Sreenivasan, R. Cohen, E. Lopez, S. Havlin, and H. E. Stanley, *Int. J. Bifurcation and Chaos* **17**, 2215 (2007); L. A. Braunstein, S. V. Buldyrev, R. Cohen, S. Havlin, and H. E. Stanley, *Phys. Rev. Lett.* **91**, 168701 (2003).
- [22] Here t represent the number of simulation steps of the building process, each of which consists of selecting a single open link belonging to the aggregate and connect it to another link (cases (i), (ii), (iii) shown in Fig. 1).
- [23] If $r = r_l$ corresponding to a certain shell ℓ , $r = \sum_k P_\ell(k)$ and $P_r(k) = P_\ell(k)/r$ in notations of Ref. [11].
- [24] $\Lambda(t_\ell)N = \Lambda_\ell(t_\ell)N$ coincides with χ_ℓ in notations of Ref. [11].
- [25] For different realizations from different root, the results shown in Fig. 3 and Fig. 4 are aligned nicely along the same line. There are almost no deviations.
- [26] M. Bogañá, R. Pastor-Satorras, and A. Vespignani, *Eur. Phys. J. B* **38**, 205 (2004).
- [27] S. Dubuc, *Ann. Inst. Fourier* **21**, 171 (1971).
- [28] R. Cohen, K. Erez, D. ben-Avraham, and S. Havlin, *Phys. Rev. Lett.* **85**, 4626 (2000); *Ibid.* **86**, 3682 (2001).
- [29] J.-P. Hansen and I.R. McDonald, *Theory of Simple Liquids*, 2nd ed., Academic Press, London, 1986.

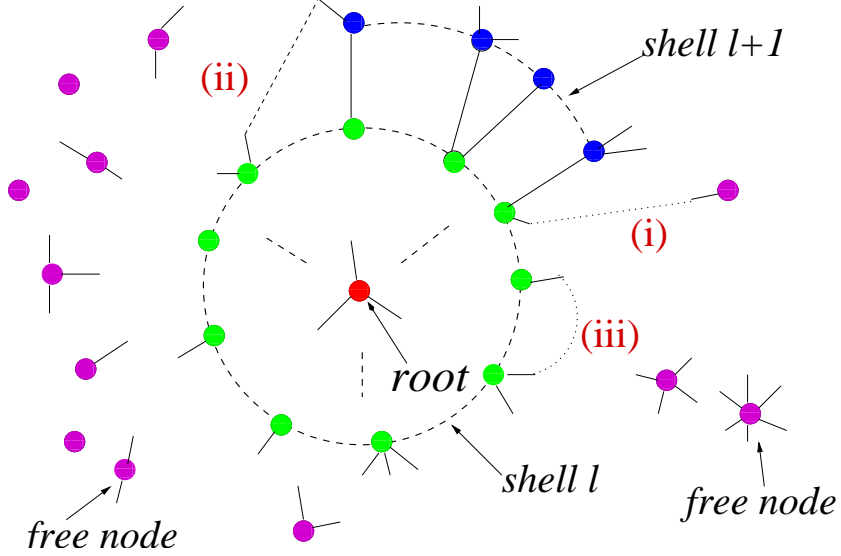


FIG. 1: (color online) Building the network begins from a randomly chosen node (root), shown in red at the center of the figure. This schematic illustration shows the network during the building of shell $\ell + 1$. We do not start to build shell $\ell + 1$ until shell ℓ is completed. All the nodes which are already included in shell $\ell + 1$ are shown in blue, while the free nodes not yet connected in shell $\ell + 1$ are shown in purple. At a certain time step, in order to connect an open link from shell ℓ to another open link, we must consider three scenarios: (i) Connecting to an open link taken from a free node. (ii) Connecting to an open link from shell $\ell + 1$. (iii) Connecting to another open link from shell ℓ . This way the aggregate keeps growing shell after shell until all the open links are connected. Note that in scenarios (ii) and (iii) there is a chance to create parallel links (two links connecting a pair of nodes) and circular links (one link with two ends connected to the same node). For a large network with a finite \tilde{k} , such events occur with a negligible probability.

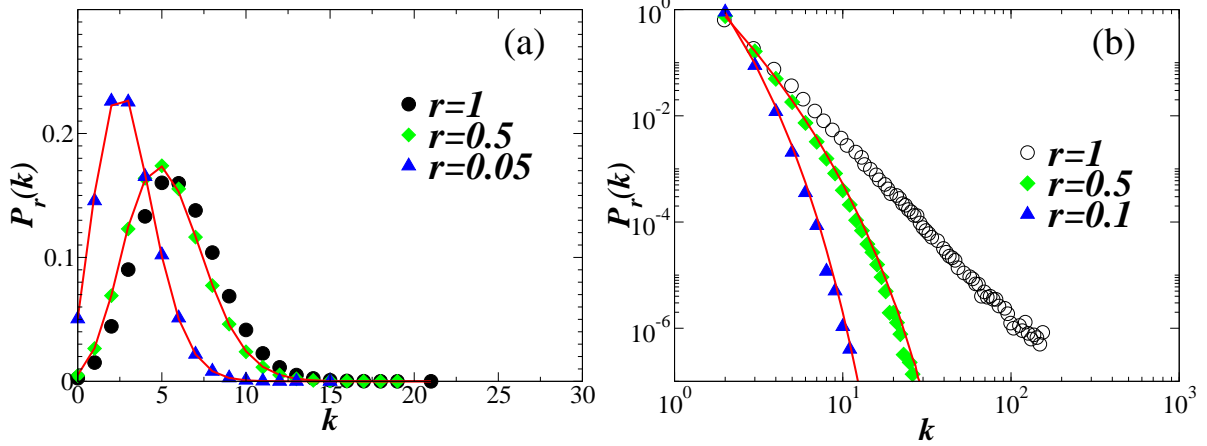


FIG. 2: The degree distribution, $P_r(k)$, in E_r for (a) an ER network with $N = 10^6$, $\langle k \rangle = 6$ and $r = 1, 0.5$ and 0.05 . The simulation results (symbols) agree very well with the theoretical predictions (lines) of Eq.(22). (b) a SF network with $\lambda = 3.5$, $k_{\min} = 2$ and $N = 10^6$, $P_r(k)$ with $r = 1, 0.5$ and 0.1 . The simulation results shown by symbols fit well with the theoretical predictions of Eq.(16). For a SF network, we compute Eq.(16) numerically using the $P(k)$ obtained from the generated network.

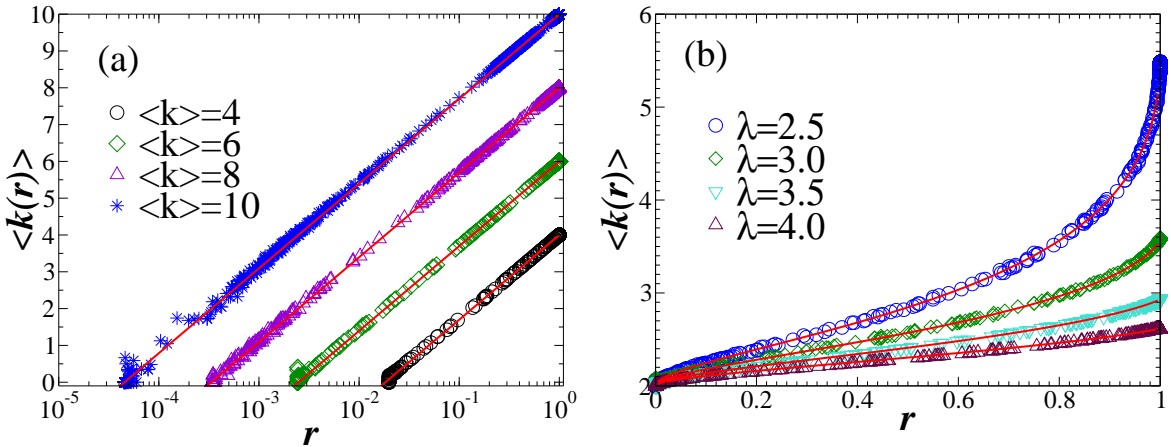


FIG. 3: Average degree $\langle k(r) \rangle$ of the nodes in E_r as a function of r for (a) four ER networks with different values of $\langle k \rangle$, and (b) four SF networks with $k_{\min} = 2$ and different values of λ . The symbols represent the simulation results for ER and SF networks of size $N = 10^6$. The lines in (a) represent Eq.(21). The lines in (b) are the numerical results of Eq.(17), using the degree distribution obtained from the networks.

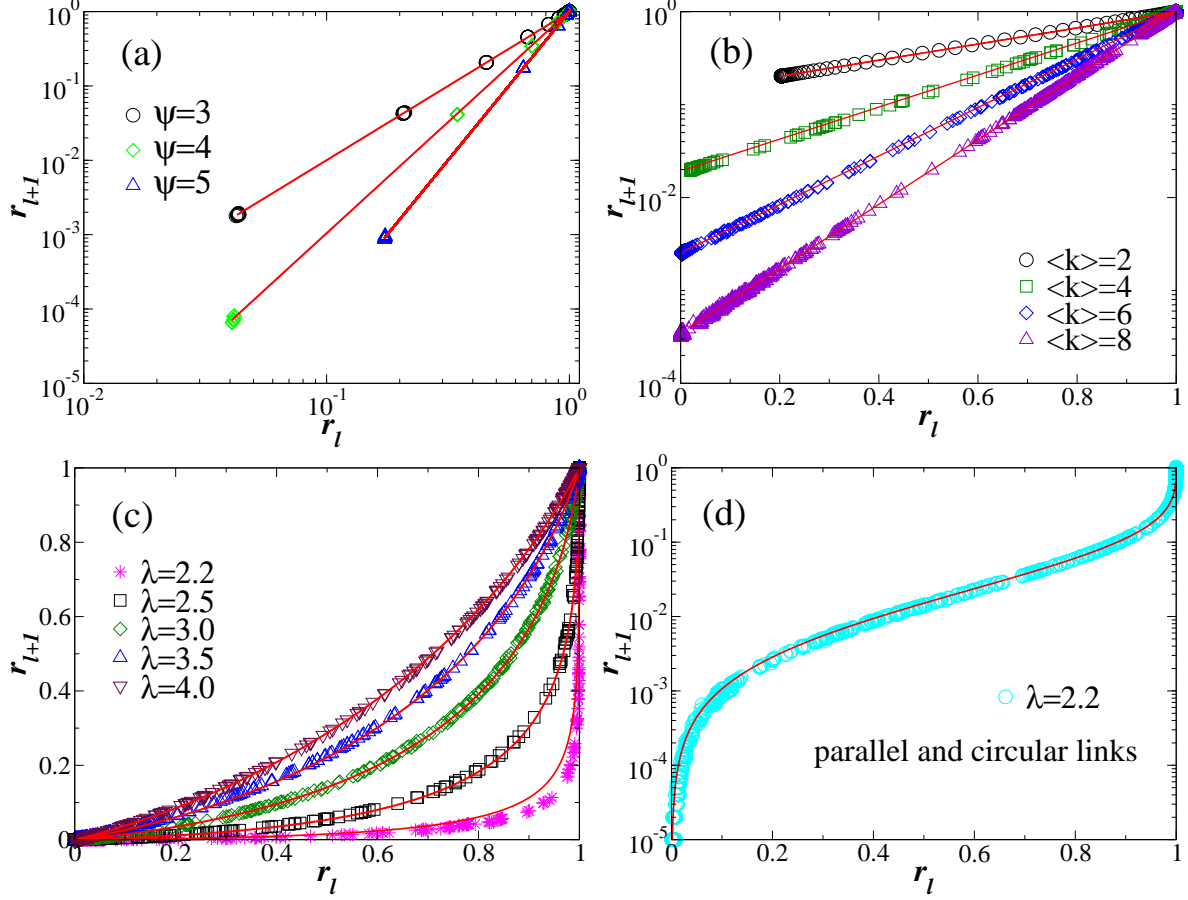


FIG. 4: (Color online) For a randomly chosen root in the network, the fraction of nodes $r_{\ell+1}$ in $E_{\ell+1}$ as a function of the the fraction of nodes r_ℓ in E_ℓ for (a) three RR networks of size $N = 10^5$ with different ψ . The red lines represents the theoretical prediction of Eq.(35). (b) Four ER networks of size $N = 10^5$ with different $\langle k \rangle$. The red lines represent the theoretical predictions of Eq.(36). (c) Five SF networks of size $N = 10^5$ with different values of λ . The red lines shown are the numerical results of Eq.(34) using the degree distribution obtained from the simulation. For $\lambda \geq 2.5$, the agreement between the theory [Eq.(34)] and the simulation results is perfect. (d) A SF network of size $N = 10^5$ with $\lambda = 2.2$, which allows parallel and circular links (PCL) during its construction. Simulation results of SF networks with PCL show excellent agreement with the theory (full line).

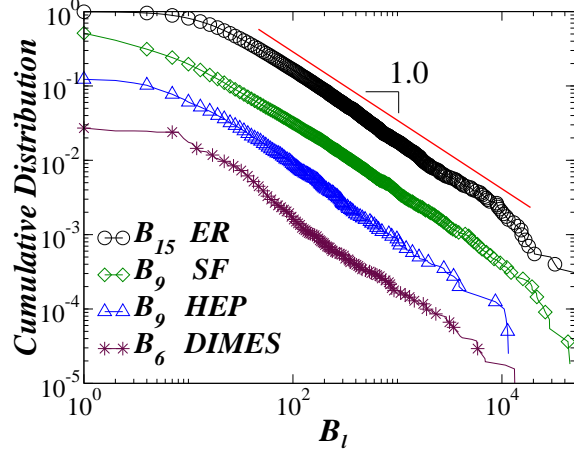


FIG. 5: Cumulative distribution function of $P(B_\ell)$, of the number of nodes B_ℓ in shell ℓ ($\ell \gg d$) for an ER network with $\langle k \rangle = 4$, $N = 10^6$ and $d \approx 10.0$, a SF network with $\lambda = 2.5$, $N = 10^6$ and $d \approx 4.7$, the HEP network ($d \approx 4.2$) and the DIMES network ($d \approx 3.3$). Note that slope -1 of the cumulative distribution function implies $P(B_\ell) \sim B_\ell^{-2}$, which holds for all four examples, as well as for many other networks studied [14].

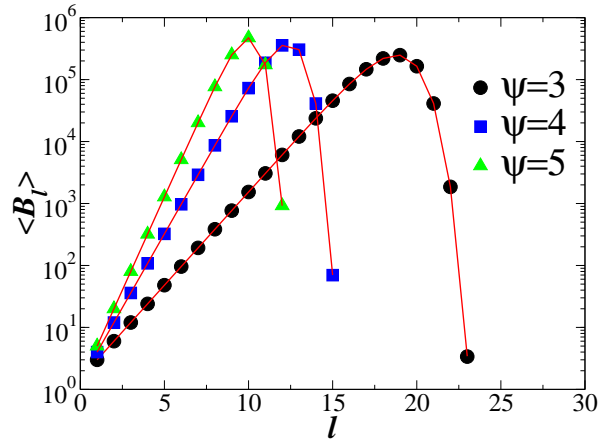


FIG. 6: The average number of nodes, $\langle B_\ell \rangle$, in shell ℓ as a function of the shell index ℓ for the RR network with different ψ . The theoretical predictions (full lines) calculated from Eq.(52) and Eq.(53) fit very well the simulation results (symbols).

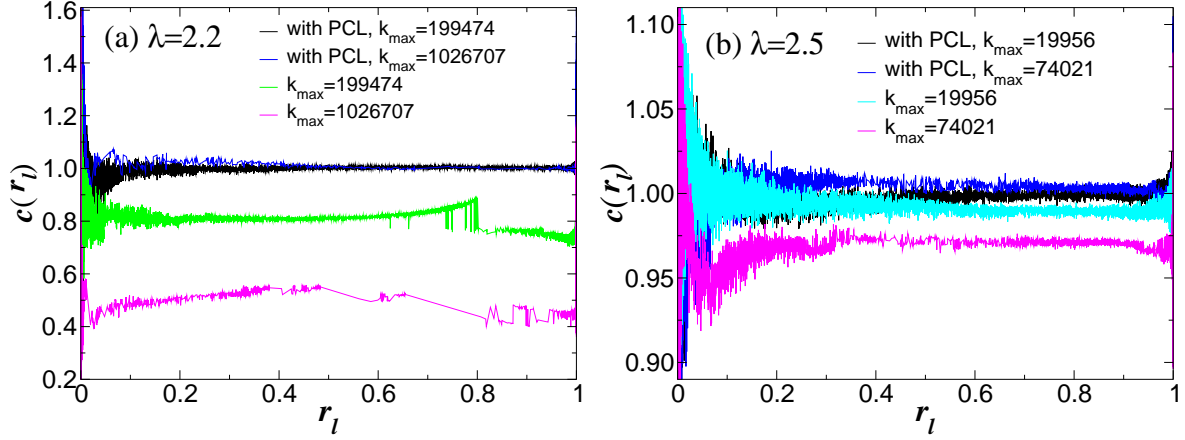


FIG. 7: $c(r_\ell)$ for SF networks. (a) The case $\lambda = 2.2$. Values of k_{\max} equal and larger than the natural cutoff ($k_{\max} = k_{\min} N^{1/(\lambda-1)} \approx 2 \times 10^5$) are compared for networks with and without parallel and circular links (PCL). Notice that, the discontinuity of the lines is due to the existence of the large degree nodes. (b) The case $\lambda = 2.5$. Similarly, values of k_{\max} equal and larger than the natural cutoff ($k_{\max} \approx 2 \times 10^4$) are compared for networks with and without PCL.

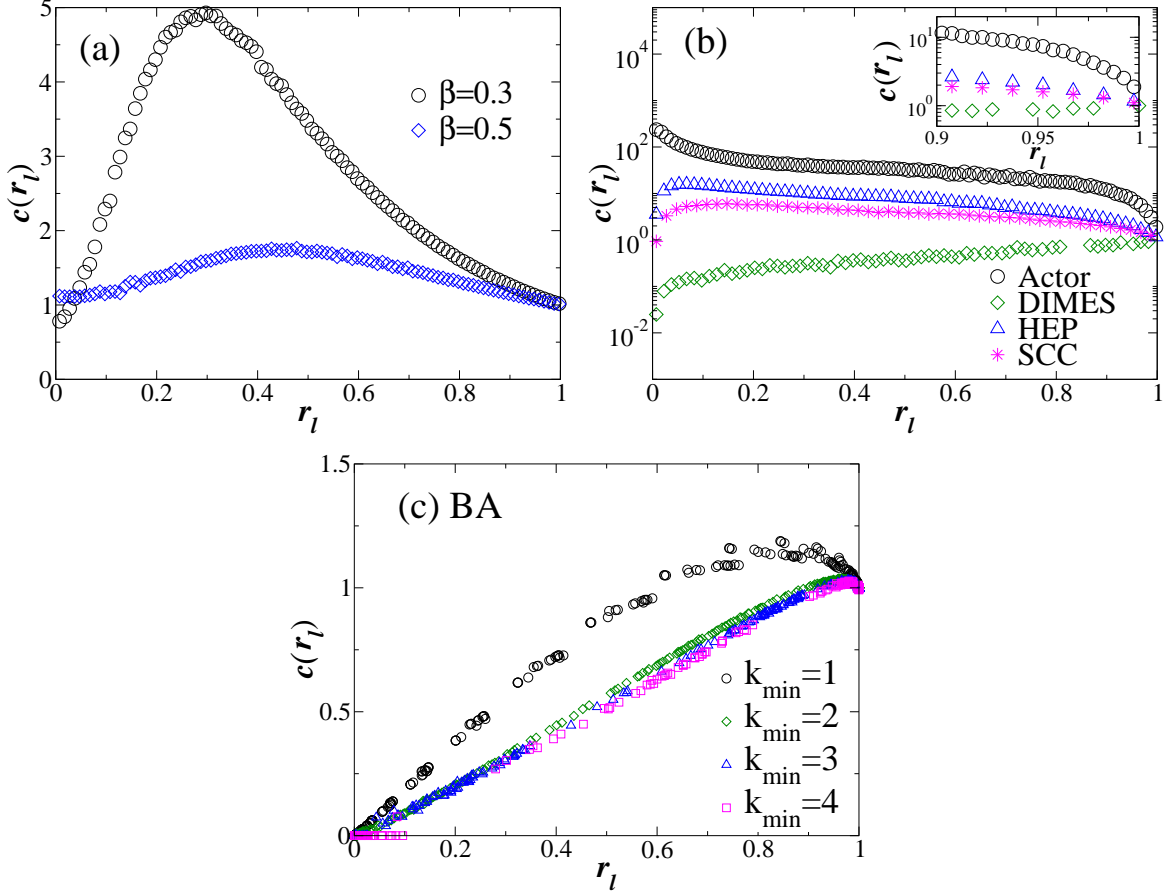


FIG. 8: $c(r_\ell)$ for various networks. (a) WS network with $\psi = 4$ and $\beta = 0.3$ and 0.5 . (b) Four real networks: Actor collaboration network (Actor), High Energy Physics citations network (HEP), AS Internet network (DIMES), and Supreme Court Citation network (SCC). In the insert we show the enlarged area of $r > 0.9$. (c) BA networks of size $N = 10^6$ with different k_{\min} .

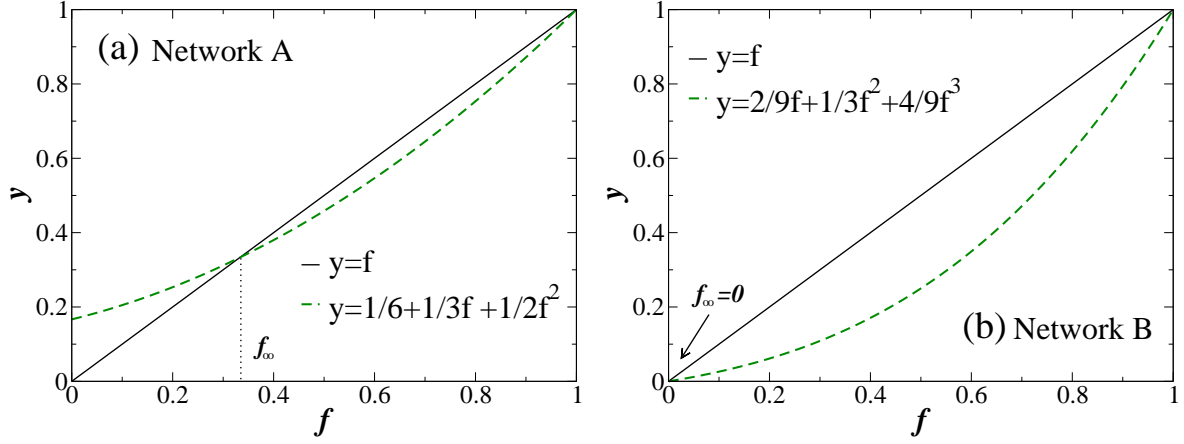


FIG. 9: Plots of both sides of Eq.(31) for (a) Network A, with equal probability of having degree 1, 2 and 3, and (b) Network B, with equal probability of having degree 2, 3 and 4. For network A, a non-zero solution f_∞ can be seen. For network B, $f_\infty = 0$ is the solution of Eq.(31).